Diabetologia (2005) 48: 1627–1636
DOI 10.1007/s00125-005-1819-y

ARTICLE

C. P. Hodgkinson · A. Mander · G. J. Sale

Protein kinase-ζ interacts with munc18c: role in GLUT4 trafficking

Received: 21 December 2004 / Accepted: 9 March 2005 / Published online: 29 June 2005

Abstract *Aims/hypothesis:* Insulin-stimulated glucose transport requires a signalling cascade through kinases protein kinase (PK) Cζ/λ and PKB that leads to movement of GLUT4 vesicles to the plasma membrane. The aim of this study was to identify missing links between the upstream insulin-regulated kinases and the GLUT4 vesicle trafficking system. *Materials and methods:* A yeast two-hybrid screen was conducted, using as bait full-length mouse munc18c, a protein known to be part of the GLUT4 vesicle trafficking machinery. *Results:* The yeast two-hybrid screen identified PKCζ as a novel interactor with munc18c. Glutathione S transferase (GST) pull-downs with GST-tagged munc18c constructs confirmed the interaction, mapped a key region of munc18c that binds PKCζ to residues 295–338 and showed that the N-terminal region of PKCζ was required for the interaction. Endogenous munc18c was shown to associate with endogenous PKCζ in vivo in various cell types. Importantly, insulin stimulation increased the association by approximately three-fold. Moreover, disruption of PKCζ binding to munc18c by deletion of residues 295–338 of munc18c or deletion of the N-terminal region of PKCζ markedly inhibited the ability of insulin to stimulate glucose uptake or GLUT4 translocation. *Conclusions/interpretation:* We have identified a physiological interaction between munc18c and PKCζ that is insulin-regulated. This establishes a link between a kinase (PKCζ) involved in the insulin signalling cascade and a known component of the GLUT4 vesicle trafficking pathway (munc18c). The results indicate that PKCζ regulates munc18c and suggest a model whereby insulin triggers the docking of PKCζ to munc18c, resulting in enhanced GLUT4 translocation to the plasma membrane.

C. P. Hodgkinson · A. Mander · G. J. Sale (✉)
School of Biological Sciences, University of Southampton,
Biomedical Sciences Building, Bassett Crescent East,
Southampton, SO16 7PX, UK
e-mail: G.J.Sale@soton.ac.uk
Tel.: +44-23-80594307
Fax: +44-23-80594459

Keywords Glucose transport · GLUT4 · Insulin · munc18c · Protein kinase C

Abbreviations ATCC: American Type Culture Collection · CHO-*myc*Glut4 cells: CHO cell line expressing *myc*-tagged Glut4 · DAG: diacylglycerol · FL: full length · GST: glutathione S transferase · HA: haemagglutinin · munc18cΔPKCζ: munc18c FL with the PKCζ-interaction site deleted · munc18c FL: full-length mouse munc18c · PKC: protein kinase C · PKCζ-cat: a catalytically active construct unable to bind munc18c · SNAP-23: synaptosome-associated protein of 23,000 Da · v-SNARE: soluble *N*-ethylmaleimide-sensitive factor attachment protein receptor · VAMP: vesicle-associated membrane protein

Introduction

One of the major effects of insulin is to promote the influx of glucose into cells. This is achieved by activation of a signalling cascade and the trafficking of a vesicle containing the glucose transporter GLUT4 to the plasma membrane. Several kinases involved in insulin-stimulated glucose transport have been discovered, namely, protein kinase (PK) Cζ/λ [1, 2] and PKB [3, 4]. CAP-Cbl has also been implicated in insulin-stimulated glucose transport [5, 6]. GLUT4 vesicle trafficking is similar to that seen in synaptic vesicles. The GLUT4 vesicle contains the soluble *N*-ethylmaleimide-sensitive factor attachment protein receptor (v-SNARE) vesicle-associated membrane protein (VAMP)-2, which binds to the t-SNARE complex containing syntaxin-4 and synaptosome-associated protein of 23,000 Da (SNAP-23) found in the plasma membrane [7–9]. Several proteins have been proposed to act to regulate the interaction between syntaxin-4 and VAMP-2. These proteins are synip [10] and munc18c [11–13]. Munc18c, also known as munc18-3, has two homologues, munc18a (munc18-1) and munc18b (munc18-2). Munc18a is found in neurons where it inhibits the association of VAMP-1 and SNAP-25 with syntaxin-1 [14]. Likewise,

munc18c binds to syntaxin-4, and as this association is stronger than that between VAMP-2 and syntaxin-4 [11–13], it acts as a clamp preventing the GLUT4 vesicle binding to the plasma membrane in the basal state. When stimulated by insulin this clamp is removed by an unknown mechanism and the GLUT4 vesicle docks with the plasma membrane. Displaced munc18c may also be involved in fusing the GLUT4 vesicle to the plasma membrane [7, 15]. It remains to be seen whether any component of the insulin signalling cascade regulates munc18c.

Atypical PKCs are known to mediate signalling responses either by phosphorylating targets or by binding other proteins. The aPKC V1 sequence in the regulatory domain and other domains of PKCζ is clearly important in binding proteins that regulate apoptosis and cell polarity such as p62, Par-4, Par-6 and ASIP [16–19]. The failure to discover relevant phosphorylated substrates for the atypical PKCs increases the prospect that enhancement of glucose transport involves scaffolding links.

In the present study we have identified that PKCζ interacts with munc18c. This interaction was enhanced by insulin, indicating that the association was specific. Studies with munc18c and PKCζ constructs unable to bind to each other suggested that binding of PKCζ to munc18c may alleviate the clamping action of munc18c and thereby facilitate increased GLUT4 translocation to the plasma membrane.

Materials and methods

Yeast two-hybrid system The LexA yeast two-hybrid system and the human matchmaker brain cDNA library were from Clontech (BD Biosciences, Oxford, UK). Full-length mouse munc18c (munc18c FL) was cloned from a mouse adipocyte cDNA library using the 5′ oligonucleotide 5′CGG CTG GGA ATT CAT GGC GCC GC3′ and the 3′ oligonucleotide 5′GAC AAC CAT CTC GAG TTA CTC AT3′ via Pfu polymerase. The primers were derived from the munc18c sequence as found in Accession number U19521 [13]. The *Eco*RI and *Xho*I sites, required for cloning into pLexA, are underlined. The constructs were ligated into pLexA (Clontech) and then sequenced. The PCR products, digested with *Eco*RI and *Xho*I, were then ligated into *Eco*RI-*Xho*I-digested pLexA to generate in-frame fusions with the LexA-binding domain, confirmed by sequencing and expression of the full-length protein in yeast. The EGY48[p8opLacZ] yeast strain was first transformed with pLexA-munc18c and tested for expression of the hybrid protein via western blotting using the LexA antibody (Clontech). Subsequently, the EGY48[p8opLacZ, pLexA-munc18c] were transformed with the pB42AD brain cDNA library (100 μg) and plated out onto SD/dex/kan/-his/-trp/-ura. After 3 days of growth, the transformants were collected and 5×10^6 plated out onto SD/gal/raf/kan/-his/-trp/-ura/-leu selection medium plates supplemented with X-gal (80 μg/ml). Leu+LacZ+ colonies were collected over a period of 5 days. Library plasmids were rescued via transformation of KC8 bacteria grown on M9TrpDOAmp plates. Putative interacting library plasmids were reintroduced into EGY48[p8opLacZ, pLexA-munc18c] as the positive control and with pLexA-laminin, pLexA-p53 as negative controls with the selection on SD/gal/raf/kan/-his/-trp/-ura/-leu/X-gal plates.

Plasmid constructs Munc18c FL was subcloned from pLexA pGex-5X-1 (Amersham, Little Chalfont, Bucks, UK). Deletions of the munc18c protein were first expressed as glutathione S transferase (GST) fusions of munc18c. Using the pGex-5X-1 munc18c FL construct as template, the deletions were amplified using Pfu. The forward primer was sequence-specific and contained an *Eco*RI site, the reverse primer was to the pGex plasmid and was 3′ of the *Xho*I site in the plasmid (5′CCG TCA TCA TCT AGA CGC GCG A3′). *Eco*RI-*Xho*I digestion of the PCR fragments facilitated in-frame cloning into pGex-5X-1. Forward primers were as follows: munc18c 295 5′ GGG TTG AAT TCC GGC ACA TCG CGG TGG TG3′, munc18c 338 5′GAT GCC GGA ATT CCG AAA GCA GAT CTC GAA3′, munc18c 381 5′GAT GCT GAA TTC CAG CGG GTG AAG GAC TC3′, munc18c 468 5′CGG TCT GCA GAA TTC ACT TTT CAG CTT TC3′, munc18c 493 5′GAT TAG AAT TCA AAG AGT GGC CGT ATT GT3′ and munc18c 558 5′GTT TCC CAG GCA CAT GAA TTC TGT GAG GTT A3′. The *Eco*RI site is underlined, the number after the munc18c refers to the first amino acid of the munc18c protein following the *Eco*RI site, thus munc18c 295 represents a munc18c truncated protein encompassing amino acid residues 295–592. A munc18c construct was produced, munc18cΔPKCζ, where the PKCζ-interaction site was deleted from the munc18c FL protein. Using munc18c FL and munc18c 338 as templates, amino acids 1–295 were amplified with a pGex forward primer 5′CAC ACA GGT ACC AGT AGT CAT GGC3′ and a munc18c sequence-specific reverse primer 5′ CCG GTG TCG AAC CCG CAC CCA3′. Amino acids 336–592 were amplified using a munc18c primer that contained the sequence for the residues 336 onwards as well as residues 290–295 (underlined) 5′GTG CGG GTT CGA CAC CGG CAC TTC CGA AAG CAG ATC TCG A3′ and a pGex reverse primer 5′CCG TCA TCA TCT AGA CGC GCG A3′. The PCR products were allowed to anneal and Pfu added to fill in the long overhangs. pGex forward and reverse primers were added and the construct amplified with Pfu. PCR product was digested with *Eco*RI and *Xho*I and cloned into pGex-5X-1. The munc18c FL, munc18c 295, munc18c 338 and munc18cΔPKCζ were subsequently subcloned into pcDNA4HisMax-C (Invitrogen, Paisley, UK), in-frame with the 6×His and Xpress epitopes. GLUT4 was amplified from a mouse clone supplied by Invitrogen (Clone ID 4207674, Accession number BC014282), which contained the full-length GLUT4 sequence. The full-length GLUT4 was amplified from the plasmid by Pfu using the primers 5′ATG CGG TCG GGT TTC CAG3′ and 5′TCA GTC ATT CAC ATC TGG C3′. The PCR product was further amplified by Pfu using the primers 5′GCA TGG AAT TCA TGC CGT CGG GTT TCC AG3′ and 5′GCT AGC TCG AGT CAG TCA TTC

ACA TCT GGC3′. Digestion of this PCR product with *Eco*RI and *Xho*I allowed ligation into pcDNA*myc* vector [20, 21], generating a GLUT4-*myc* fusion. Haemagglutinin (HA)-tagged PKCζ has been described previously [20, 21].

Transient cell transfection in COS-1 cells of HA-tagged PKCζ constructs Exponentially growing COS-1 cells [20, 21] (2×10^6) were transiently transfected using Effectene (Qiagen, Crawley, UK) and the manufacturer's protocol. After 48 h, cell lysates were prepared using lysis buffer (50 mmol/l Tris–pH 7.8, 150 mmol/l NaCl, 0.1% v/v NP-40, 1% v/v protease inhibitor cocktail [Sigma, Poole, UK]). Extracts were used immediately where required.

GST pull-down protocol BL21 cells were used to express the GST-tagged munc18c constructs. BL21 cells over-expressing GST-tagged munc18c constructs were lysed using Bugbuster (Novagen, CN Biosciences, Nottingham, UK) and clarified extracts incubated with glutathione beads (Amersham). After several washes with PBS, the glutathione bead-munc18c complex was exposed to cell extracts prepared from COS-1 cells overexpressing HA-tagged PKCζ constructs. After 4 h of constant agitation at 4°C, complexes were washed three times with PBS and then resuspended in a small volume of PBS.

Transfection into CHO cells CHO cells (CHO-K1, American Type Culture Collection [ATCC] CCL-61; LGC Promochem, Teddington, UK) were cultured in Ham's medium supplemented with 10% v/v fetal bovine serum and 1% v/v glutamine at 37°C 5% CO_2. CHO cells were made to stably express *myc*-tagged GLUT4 by standard protocols using PolyFect (Qiagen) as the transfection reagent (manufacturer's instructions). Transient transfection into a CHO cell line expressing *myc*-tagged GLUT4 (CHO-*myc*GLUT4 cells) of pcDNA4 Xpress-tagged munc18c constructs was also carried out using Polyfect.

2-Deoxyglucose transport assay This was performed in the presence and absence of 100 nmol/l insulin as previously described [22].

Membrane fractionation CHO-*myc*GLUT4 cells were fractionated using a procedure outlined previously [23].

Immunoprecipitation 3T3-L1 adipocytes were obtained and cultured as described previously [24, 25]. L6 cells were from ATCC (ATCC number CRL-1458; LGC Promochem). L6 cells were cultured in DMEM (1 g/l glucose; Invitrogen) containing 10% Myoclone fetal calf serum (Invitrogen) at 37°C in the presence of 5% CO_2 until they reached confluence, allowed to differentiate and the L6 myotubes used 5 days after confluency. Extracts from differentiated L6 myotubes or differentiated 3T3-L1 adipocytes were diluted in lysis buffer (50 mmol/l Tris–pH 7.5, 150 mmol/l NaCl, 1% v/v Sigma Protease and Phosphatase Inhibitor cocktails) to give a 500 μl final volume (500 μg) containing a polyclonal munc18c antibody (5 μl; BD Biosciences) and Protein G : protein A beads (50:50, 20 μl; Sigma). After 5 h continuous gentle agitation at 4°C, the beads were collected by pulse spin and then washed three times in lysis buffer, after which they were resuspended in PBS.

Immunoblotting Primary antibodies (c*myc* [NEB, Hitchin, UK], monoclonal HA [NEB], GST [NEB], Xpress [Invitrogen], munc18c [BD Biosciences], PKCζ [Sigma]) were used according to the manufacturer's instructions. The munc18c antibody recognised pure munc18c produced in bacteria. Blots were developed with the ECL system according to the manufacturer's instructions (Amersham) [20, 21]. Densitometric scanning of immunoblots was carried out using Phoretix software. Intensity values are arbitrary units based on the degree of grey of the pixels within the band, with white taken to be 0, 100% black as 1.

In vitro kinase assays COS-1 cells expressing HA-tagged full-length PKCζ or HA-tagged PKCζ-CB were serum-starved (24 h), stimulated with 15% serum for 15 min and extracts prepared. GST alone, GST-tagged munc18c 295, and GST-tagged munc18c 338 were overexpressed in BL21 cells and coupled to glutathione beads. COS-1 cell extracts and glutathione bead complexes were treated as described above for the GST pulldown and washed a further twice in kinase buffer lacking ATP. Samples were incubated at 30°C for 30 min in a buffer containing 50 mmol/l Tris–pH 7.5, 10 mmol/l $MgCl_2$, 12.5 μmol/l ATP, 0.185 MBq [γ-^{32}P]ATP, phosphatidylserine (200 μg/ml) and diacylglycerol (DAG [1,2-*sn*-glycerol]), 40 μg/ml. Assay conditions were linear. Samples were analysed by 10% SDS-PAGE and the GST-tagged band excised for scintillation counting.

Results

Detection of proteins binding to munc18c To identify proteins able to interact with munc18c, we employed the LexA yeast two-hybrid system to screen a human brain cDNA library. Munc18c FL was fused to the LexA DNA-binding domain of the Clontech pLexA vector and subsequently used in an interactor hunt with a brain cDNA library. Screening of 5×10^6 transformants yielded 28 Leu+LacZ+colonies. One clone was PKCζ which is the focus of this study. Experiments carried out in yeast showed robust β-galactosidase activity when munc18c and PKCζ were co-expressed. When laminin or p53 was substituted for munc18c no β-galactosidase activity was seen (Fig. 1a). Thus the interaction between munc18c and PKCζ was a true positive.

Determination of the domains of PKCζ and munc18c that interact To further validate the interaction between PKCζ and munc18c seen in the yeast two-hybrid screen and to elucidate the nature of the domains on the two proteins that interacted, GST pull-down assays were performed. For this, purified GST-tagged munc18c constructs were coupled to glutathione beads and incubated with extracts

of COS-1 cells transfected with HA-tagged PKCζ constructs. Complexes were washed to remove non-specific binding, separated by SDS-PAGE and immunoblotted with anti-HA antibodies to test for precipitation of the HA-tagged PKCζ constructs. As is shown in the top panel of Fig. 1c, lane 2, PKCζ associated with munc18c FL. PKCζ was not precipitated when extracts were incubated with GST coupled to glutathione beads (Fig. 1c, top panel, lane 1) indicating that the association between PKCζ and munc18c was specific. To determine which regions of munc18c were responsible for the interaction with PKCζ,

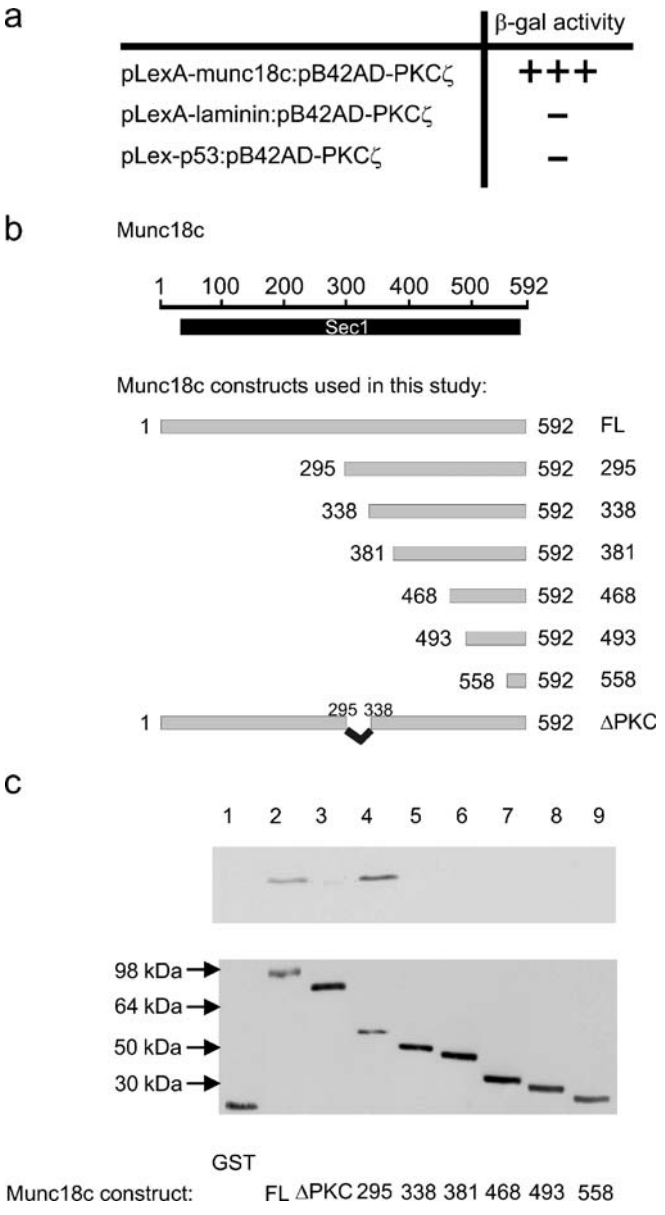

Fig. 1 PKCζ interacts with munc18c in yeast and in vitro. **a** The yeast reporter strain was co-transfected with PKCζ and various LexA constructs. Transformant yeasts were assayed for growth on leucine-deficient medium and for β-galactosidase (β-gal) activity after 5 days. +++ refers to the Leu+LacZ+ phenotype showing robust β-galactosidase activity and representing a two-hybrid interaction; –indicates no interaction as shown by no β-galactosidase activity. **b** Munc18c is a 592 amino-acid-long protein. A homology search shows that the protein contains a Sec1 domain. The munc18c constructs used in this study are shown. **c** COS-1 cells were transiently transfected with PKCζ (expressed as HA fusions). Munc18c constructs, expressed as GST fusions (*bottom panel*), were coupled to glutathione beads. Cell extracts were incubated with the glutathione bead complexes, and after extensive washing, proteins were separated by SDS-PAGE, transferred to a nitrocellulose membrane, and probed for HA to detect coprecipitated PKCζ (*top panel*). The results are representative of four independent experiments

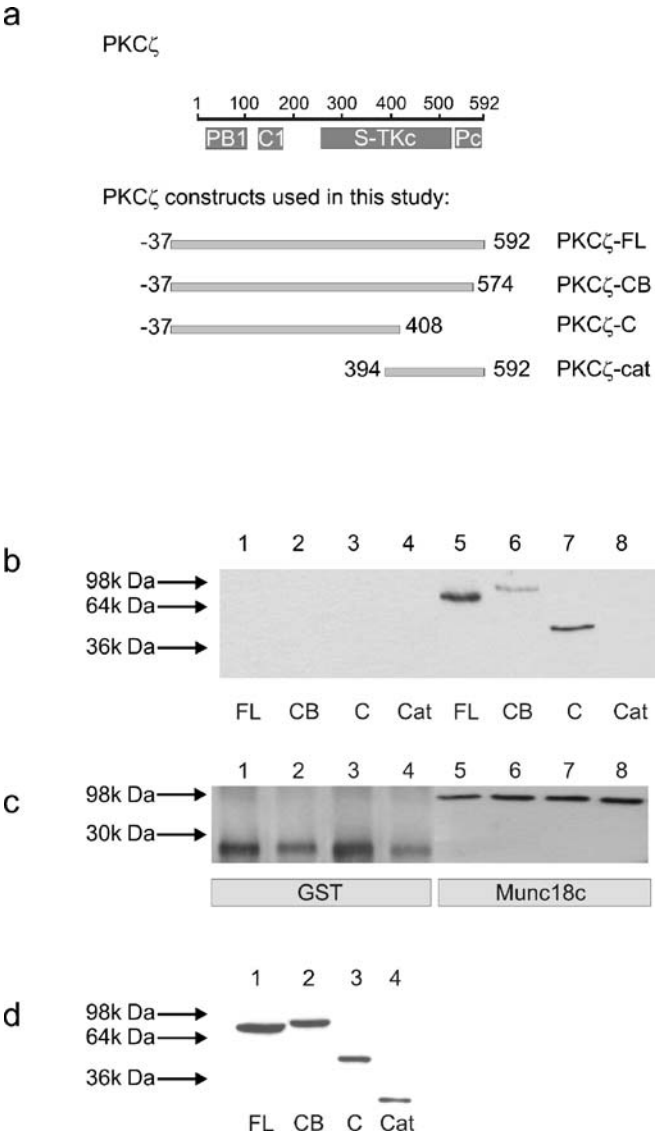

Fig. 2 Munc18c requires the N-terminal portion of PKCζ for interaction. PKCζ contains several domains, namely, PB1, C1 which binds to DAG, a kinase domain (S-TKc) and PKC-terminal domain (Pc) as shown in (**a**). COS-1 cells were transiently transfected (**a**) with several HA-tagged PKCζ constructs. Munc18c FL, expressed as a GST fusion, was coupled to glutathione beads. Cell extracts were incubated with the glutathione bead complexes, and after extensive washing, proteins were separated by SDS-PAGE, transferred to a nitrocellulose membrane, and probed for HA to detect coprecipitated PKCζ constructs (**b**) or GST to check for loading of the GST-tagged munc18c FL (**c**). Aliquots of the lysate were also analysed for levels of expression of the HA-tagged PKCζ constructs using HA antibody (**d**). The results are representative of two independent experiments

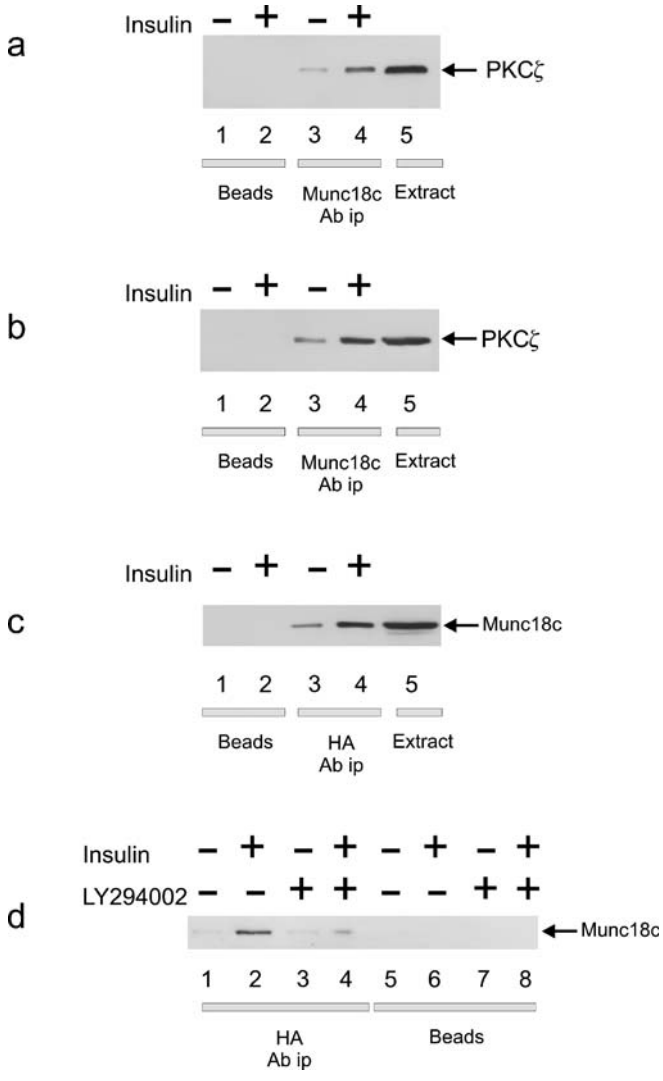

◀ **Fig. 3** Insulin-regulated association between PKCζ and munc18c in vivo. **a** (3T3-L1 adipocytes) and **b** (L6 myotubes) show that endogenous PKCζ and endogenous munc18c associate. Cells were serum-starved for 24 h and then incubated for 5 min in the presence or absence of 100 nmol/l insulin. Endogenous munc18c was immunoprecipitated from cell lysates (0.5 mg protein) and the immunoprecipitates extensively washed. Proteins in the immunocomplex were immunoblotted with a PKCζ antibody. Control immunoprecipitations containing an equal amount of cell lysate and protein A : protein G beads but omitting the munc18c antibody were also carried out. Lane 5 contains cell extract (1% of immunoprecipitation input). The results are representative of two independent experiments. **c** CHO cells overexpressing HA-tagged PKCζ were serum-starved for 24 h and then incubated for 5 min in the presence or absence of 100 nmol/l insulin. HA-tagged PKCζ was immunoprecipitated from cell lysates (0.5 mg protein) using an HA antibody and the immunoprecipitates extensively washed. Proteins in the immunocomplex were immunoblotted with a munc18c antibody. Control immunoprecipitations containing an equal amount of cell lysate and protein A : protein G beads but omitting the HA antibody were also carried out. Lane 5 contains cell extract (1% of immunoprecipitation input). The results are representative of two independent experiments. **d** CHO cells overexpressing HA-tagged PKCζ were serum-starved for 24 h, and pre-incubated with LY294002 (10 μmol/l for 1 h) after which time the cells were incubated for 5 min in the presence or absence of 100 nmol/l insulin. HA-tagged PKCζ was immunoprecipitated from cell lysates (0.5 mg protein) using an HA antibody and the immunoprecipitates extensively washed. Proteins in the immunocomplex were immunoblotted with a munc18c antibody. Control immunoprecipitations containing an equal amount of cell lysate and protein A : protein G beads but omitting the HA antibody were also carried out. The results are representative of two independent experiments

various GST-tagged deletion mutants of munc18c (see Fig. 1b) were employed in similar experiments. Munc18c 295 was found to associate with PKCζ (Fig. 1c, top panel, lane 4). Munc18c 338, 381, 468, 493 and 558 did not bind PKCζ (Fig. 1c, top panel, lanes 5–9). These results indicated that residues 295 and 338 of munc18c represented a key domain to which PKCζ bound. To test this further, a munc18c construct that lacked just residues 295–338 was employed (munc18cΔPKCζ). This construct failed to bind PKCζ, clearly showing that a key region to which PKCζ bound was between residues 295 and 338 of munc18c (Fig. 1c, top panel, lane 3). Experiments with a number of other PKC isoforms, both classic and novel, as further controls showed that these isoforms did not significantly interact with munc18c, further showing that the interaction between munc18c and PKCζ was specific (data not shown).

Experiments were then conducted to investigate the domain(s) within PKCζ required for binding to munc18c. COS-1 cells were transfected with various HA-tagged deletion mutants of PKCζ (see Fig. 2a). Lysates were incubated with purified GST-tagged munc18c FL coupled to glutathione beads. Complexes were immunoblotted with anti-HA antibodies to test for precipitation of HA-tagged PKCζ constructs. A strong band was observed with full-length PKCζ, PKCζ-CB and PKCζ-C (Fig. 2b, lanes 5–7) whereas PKCζ-cat, a catalytically active construct unable to bind munc18c, failed to bind (Fig. 2b, lane 8). These results indicate that the C-terminal portion of PKCζ is not required for interaction and that the key binding domains are in the remaining N-terminal portion of PKCζ.

Endogenous munc18c associates with endogenous PKCζ

It was important to test whether the interaction between munc18c and PKCζ occurred with the endogenous proteins in vivo. This was carried out in 3T3-L1 adipocytes and L6 myotubes. These are cell types which are known to be good models of insulin signalling in fat and muscle cells. Cells (untransfected) were lysed and the lysates incubated with a munc18c antibody to precipitate endogenous munc18c. The immunoprecipitates were then probed with a PKCζ antibody. As shown in Fig. 3, precipitation of endogenous munc18c resulted in the co-immunoprecipitation of endogenous PKCζ. Control experiments omitting the munc18c antibody confirmed the absence of PKCζ (Fig. 3). Stimulation of 3T3-L1 adipocytes or L6 myotubes with insulin significantly increased the association between munc18c and PKCζ by approximately three-fold (Fig. 3). The observation that binding between PKCζ and munc18c was markedly enhanced by insulin provided excellent further evidence that the association between the two proteins was specific. Moreover, the insulin regulation of

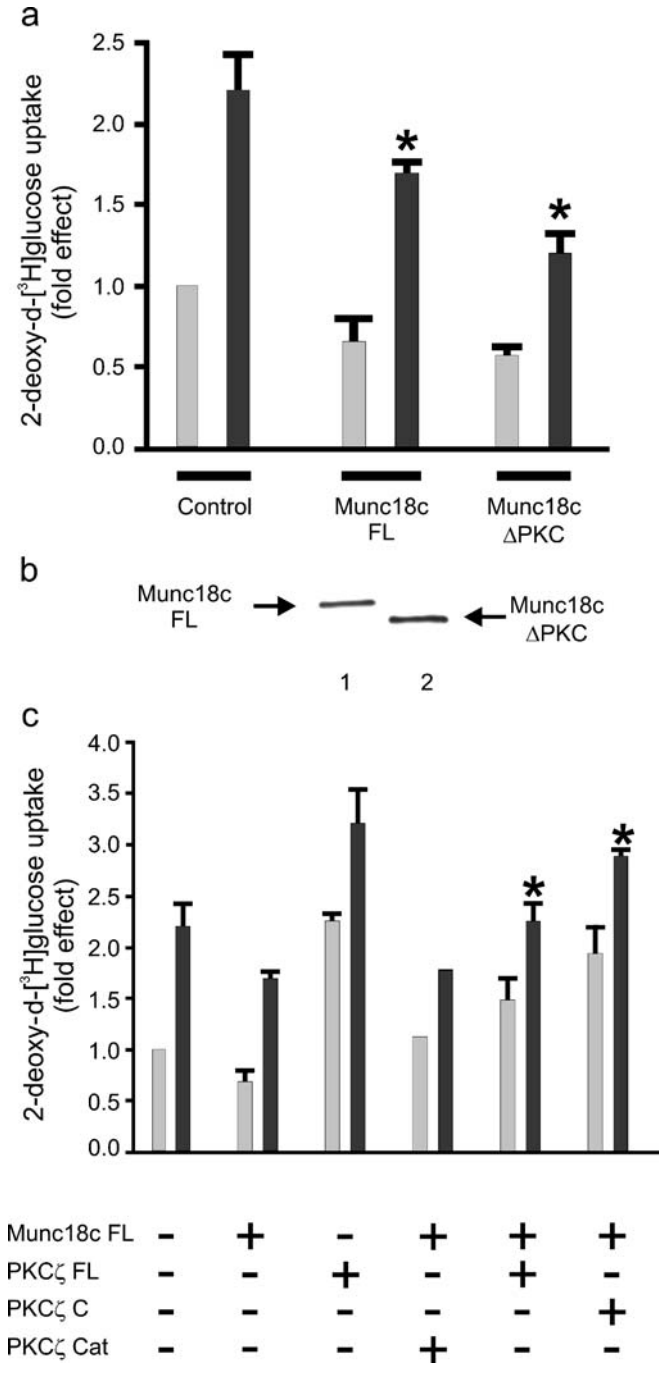

◀ **Fig. 4** Munc18cΔPKC inhibits insulin-stimulated glucose uptake. **a** CHO-*myc*GLUT4 cells were transiently transfected with the indicated Xpress-tagged munc18c construct. Cells were serum starved for 16 h then incubated in the presence (black bar) or absence (grey bar) of 100 nmol/l insulin for 20 min and the rates of 2-deoxy-D-[^{3}H]glucose uptake determined. Uptake is shown as fold effect, where glucose uptake in control cells unstimulated with insulin was taken to be 1. Results are expressed as the means±SEM of four to eight independent experiments. Results significantly different from control values and from one another are marked with an asterisk (Student's *t*-test 95% confidence level $p<0.010$). **b** Immunoblot of extracts of CHO-*myc*GLUT4 cells expressing Xpress-tagged munc18c FL (lane 1) or Xpress-tagged munc18cΔPKC (lane 2); 20 μg were loaded into each well. **c** CHO-*myc*GLUT4 cells were transiently transfected with the indicated Xpress-tagged munc18c construct and/or the indicated HA-tagged PKCζ constructs. Cells were serum starved for 16 h then incubated in the presence (black bar) or absence (grey bar) of 100 nmol/l insulin for 20 min and the rates of 2-deoxy-D-[^{3}H]glucose uptake determined. Uptake is shown as fold effect, where glucose uptake in control cells unstimulated with insulin was taken to be 1. Results are expressed as the mean of two independent experiments or the means±SEM of three to nine independent experiments. Results significantly different from control munc18c FL values are marked with an asterisk (Student's *t*-test 95% confidence level $p<0.010$). The expression level of the HA-tagged PKCζ constructs was similar (data not shown). Co-expression did not affect expression levels of munc18c (data not shown)

the binding provides a mechanism for delivery of an insulin signal to munc18c.

The insulin-stimulated association was confirmed by expressing HA-tagged PKCζ in CHO cells and then immunoprecipitating the PKCζ with an HA antibody. Munc18c was present in the immunoprecipitates. Again insulin markedly increased the association (Fig. 3c). The insulin-stimulated association was largely prevented by the phosphatidylinositol 3-kinase inhibitor, LY294002 (Fig. 3d, lanes 2 and 4).

Removal of the munc18c PKCζ-interaction site inhibits insulin-stimulated glucose uptake To investigate the role of the interaction between PKCζ and munc18c, we generated CHO-*myc*GLUT4 cells. Such cells are known to show insulin-stimulated glucose transport and to share many similarities with 3T3-L1 adipocytes, a canonical cell line used to investigate insulin-stimulated glucose transport [26, 27]. The cells were cultured in DMEM as this has been shown to be required for insulin-responsive trafficking [27]. We first generated *myc*-tagged GLUT4 and confirmed its functionality using COS-1 cells. Thus expression of the *myc*-tagged GLUT4 in COS-1 cells increased glucose uptake by 10-fold when compared with untransfected cells (data not shown). The *myc*-tagged GLUT4 was then expressed in CHO cells. This resulted in a marked enhancement in insulin-stimulated levels of glucose transport compared with wild-type CHO cells (data not shown). The level of insulin stimulation of glucose uptake in the CHO-*myc*GLUT4 cells was approximately 2.5-fold (Fig. 4a), which accorded well with the published literature on insulin-stimulated trafficking of GLUT4 to the plasma membrane of CHO cells [27]. Transient transfection of Xpress-tagged munc18c constructs was then carried out to test if they modulated glucose uptake in response to insulin. Cells expressing the Xpress-tagged munc18c constructs grew to confluency in the same way as control cells, so that there were no general cytotoxic effects associated with expression of the constructs. Munc18c FL significantly inhibited insulin-stimulated glucose uptake compared with control cells (Fig. 4a). This confirms findings in other cell types and supports the proposed clamp action role for munc18c. Co-expression of full-length PKCζ and munc18c FL rescued the inhibitory effect of munc18c (Fig. 4c). This

confirms that the expressed munc18c FL was not acting non-specifically to cause a general impairment of glucose uptake. PKCζ-cat failed to rescue (Fig. 4c). Thus insulin-stimulated glucose uptake was similar in cells expressing munc18 FL alone and those expressing both munc18c FL and PKCζ-cat. Another PKCζ construct that could associate with munc18c, PKCζ-C, also rescued cells from the inhibitory effect of expressing munc18c FL (Fig. 4c). To further evaluate the function of binding between PKCζ and munc18c, the munc18cΔPKC construct was used. Munc18cΔPKC lacks residues 295–338 and the ability to bind PKCζ. Overexpression of munc18cΔPKC significantly inhibited insulin-stimulated glucose transport compared with cells overexpressing munc18c FL and control cells (Fig. 4a). This was not due to any differences in the expression of the two constructs (Fig. 4b).

Removal of the munc18c PKCζ-interaction site inhibits insulin-stimulated GLUT4 translocation To test if the results observed in the glucose transport assay reflected translocation of GLUT4, the distribution of *myc*-tagged GLUT4 was determined in CHO-*myc*GLUT4 cells. As expected, in control cells, insulin increased the amount of plasma membrane-associated *myc*-tagged GLUT4 (Fig. 5, bars 1 and 2) and caused a concomitant decrease in the level of *myc*-tagged GLUT4 in the low-density microsome fraction (data not shown). There was no apparent effect on the level of *myc*-tagged GLUT4 in the high-density microsome fraction (data not shown). Expression of the Xpress-tagged munc18c FL construct significantly inhibited the insulin-stimulated appearance of *myc*-tagged GLUT4 in the plasma membrane (Fig. 5, bar 4). Expression of Xpress-tagged munc18cΔPKC markedly decreased the insulin-stimulated amounts of *myc*-tagged GLUT4 in the plasma membrane when compared with cells overexpressing munc18c FL (Fig. 5, bars 4 and 6). Expression of the two munc18c constructs was equivalent (e.g. Fig. 4b). These results fully support the experiments in which glucose uptake was measured.

Munc18c is phosphorylated We next considered whether munc18c was a substrate for PKCζ. For this, GST-tagged munc18c 295 or GST-tagged munc18c 338 was incubated with PKCζ in the presence of [γ-^{32}P]ATP. Munc18c 295 was significantly phosphorylated in the assay (Fig. 6, bar 2) in the presence of kinase-active PKCζ. Use of munc18c 338 resulted in significantly decreased phosphorylation (Fig. 6, bar 3). However, when PKCζ-CB, which we have shown previously to be kinase-dead [20], was substituted for kinase-active PKCζ, phosphorylation of both munc18c 295 and munc18c 338 still occurred at the same level (Fig. 6, bars 5 and 6). These results show that munc18c is robustly phosphorylated but that PKCζ is not directly responsible.

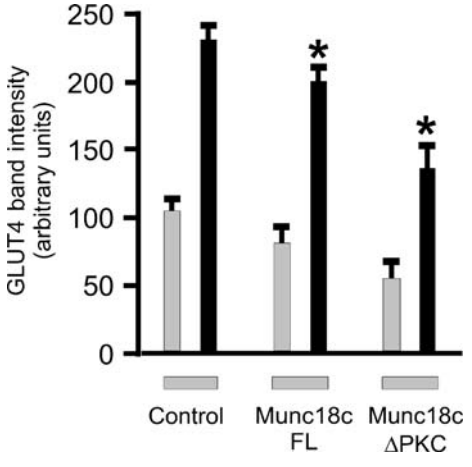

Fig. 5 Munc18cΔPKC inhibits insulin-stimulated GLUT4 translocation to the plasma membrane. CHO-*myc*GLUT4 cells were transiently transfected with the indicated Xpress-tagged munc18c construct. Cells were serum starved for 16 h then incubated in the presence (black bar) or absence (grey bar) of 100 nmol/l insulin for 20 min. Plasma membrane fractions were prepared. Fractions were probed for *myc* to detect *myc*-tagged GLUT4. Intensity values, calculated from densitometric scanning of the immunoblots, are expressed as the means±SEM of three independent experiments. Results significantly different from control values and from one another are marked with an asterisk (Student's *t*-test 95% confidence level $p<0.010$)

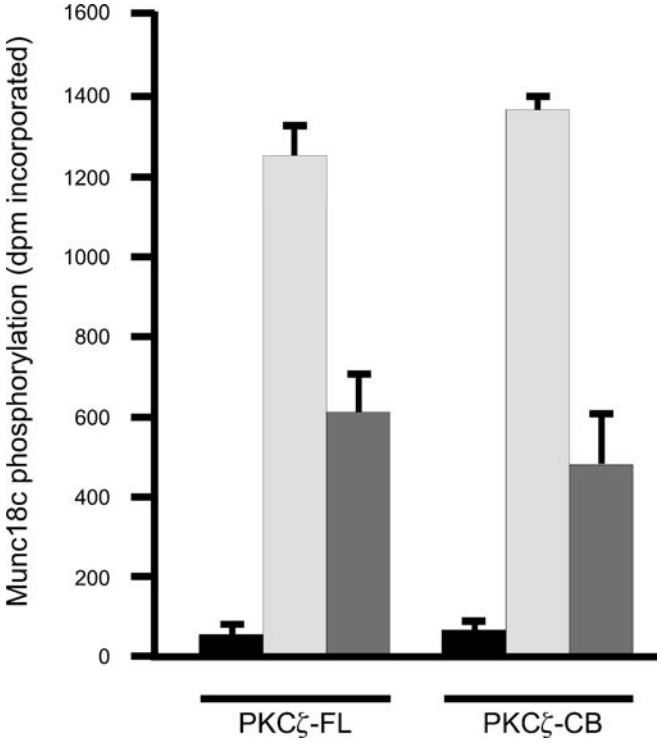

Fig. 6 Munc18c is phosphorylated. GST-tagged munc18c 295 (light grey bar), GST-tagged munc18c 338 (dark grey bar), and GST (black bar) were coupled to glutathione beads and incubated with cell extracts of COS-1 cells transiently transfected with HA-tagged full-length PKCζ (kinase-active) or HA-tagged PKCζ-CB (kinase-dead). After extensive washing complexes were incubated with [γ-^{32}P]ATP. Samples were resolved by 10% SDS-PAGE and the gel stained with Coomassie Brilliant Blue. The band corresponding to the GST construct was excised and incorporation of ^{32}P determined by scintillation counting. Results are expressed as dpm incorporated and are the means±SEM of four independent experiments

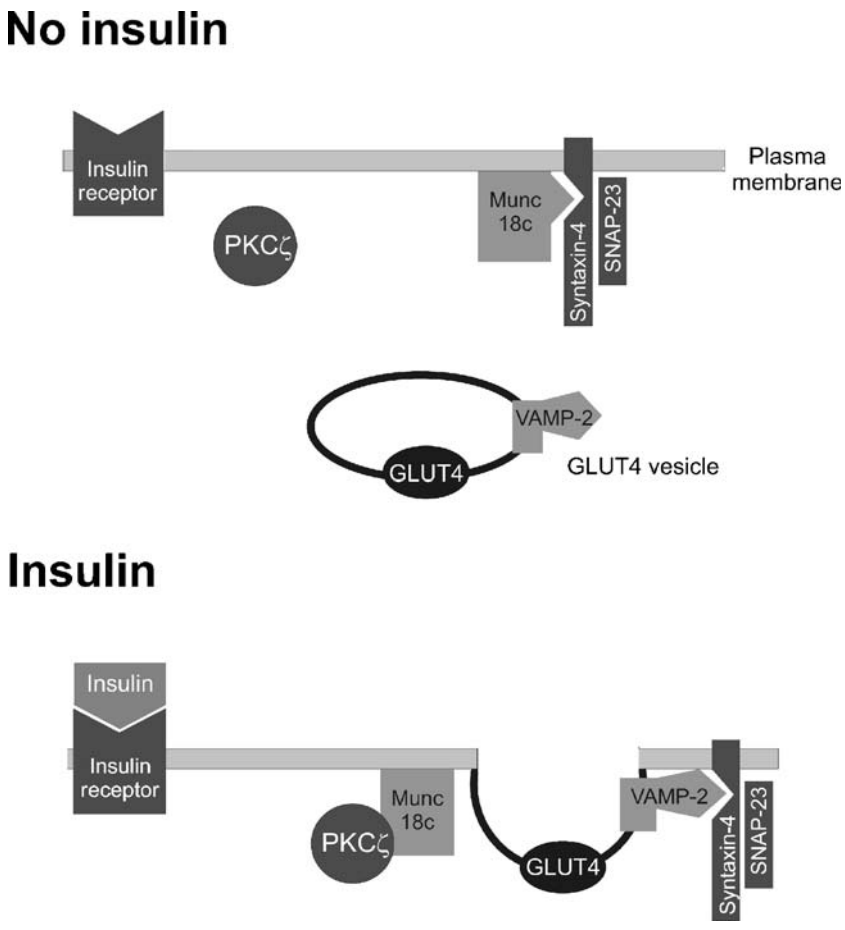

Fig. 7 Hypothetical model showing how insulin may trigger GLUT4 translocation to the plasma membrane through PKCζ and munc18c. In the absence of insulin, munc18c clamps onto syntaxin-4, preventing VAMP-2 binding. Insulin triggers docking of PKCζ with munc18c. This may induce a conformational change in munc18c so that munc18c has reduced affinity for syntaxin-4. This allows VAMP-2 to bind to syntaxin-4, thereby promoting GLUT4 vesicle fusion to the plasma membrane

Discussion

In this study we show that endogenous munc18c interacts with endogenous PKCζ and that the association is enhanced by insulin. This identifies a direct link between an insulin-regulated kinase and a component of the GLUT4 trafficking machinery.

To investigate how munc18c was regulated, we conducted a yeast two-hybrid screen with munc18c as bait to find novel interactors. This screen identified PKCζ as a true positive and thus a novel interactor with munc18c. This association merited investigation because PKCζ is one of the key enzymes regulated by insulin and has been shown to affect glucose transport through an as yet unidentified mechanism [1, 2, 28, 29]. The interaction between munc18c and PKCζ was confirmed by GST pull-downs. This approach was used to map a critical region of munc18c to which PKCζ binds to between residues 295 and 338 of munc18c. The binding of PKCζ to munc18c was specific in that it was not mimicked by classic and novel PKCs. To finally confirm the physiological nature of the interaction, the endogenous proteins were shown to interact in vivo in 3T3-L1 adipocytes and L6 myotubes, two cell lines that are major models of insulin signalling. Moreover, the interaction was increased three-fold when the cells were stimulated with insulin. This showed that the interaction was insulin-regulated and provided further very good evidence that the interaction was specific. The interaction between munc18c and PKCζ was abrogated by inhibiting phosphatidylinositol 3-kinase with LY294002. Thus stimulation of the complex formation by insulin requires signalling through phosphatidylinositol-3 kinase.

The biological function of the interaction between PKCζ and munc18c was investigated in CHO cells stably expressing *myc*-tagged GLUT4. Such cells have been used in various studies to investigate the mechanism whereby insulin stimulation promotes GLUT4 translocation to the plasma membrane [23, 26, 27, 30, 31]. The CHO cells, like 3T3-L1 adipocytes, possess GLUT4 storage vesicles which translocate to the plasma membrane in response to insulin stimulation. Overexpression of munc18c FL significantly inhibited both glucose uptake and translocation of *myc*-tagged GLUT4 to the plasma membrane, which accorded well with the published literature [11–13]. Co-expression of PKCζ constructs that associated with munc18c, but not a construct unable to bind munc18c, alleviated the inhibitory effect of munc18c on glucose uptake. To further test the function of the interaction between PKCζ and munc18c interaction, munc18cΔPKC was utilised. Munc18cΔPKC lacks residues 295–338 and thus the ability to bind PKCζ. Overexpression of munc18cΔPKC significantly inhibited insulin-stimulated glucose uptake and translocation of *myc*-tagged GLUT4 when compared with cells overexpressing

munc18c FL. This inhibition was specifically dependent on the deletion of the PKCζ-interaction site because other truncated munc18c constructs used as controls which contained the PKCζ-interaction site gave results that were identical to munc18c FL (data not shown). These results indicate that when the interaction between PKCζ and munc18c is prevented, the clamping action of munc18c is accentuated. Taken together with the observation that insulin enhances the association between endogenous munc18c and endogenous PKCζ, the results suggest a hypothetical model whereby insulin triggers the binding of PKCζ to munc18c which then relieves the clamping effect of munc18c, thereby facilitating translocation of GLUT4 to the plasma membrane (Fig. 7). This model depends on PKCζ acting through its well-known ability to exert its effects through binding to other proteins [20, 32, 33]. It is thus possible that PKCζ also delivers other regulatory proteins to munc18c. The model is based on the observations that prevention of the interaction between PKCζ and munc18c by mutating either protein at their site of interaction affects glucose uptake. While the model represents the simplest interpretation of the results, the results do not exclude the possibility that the munc18c and PKCζ mutations might also affect their binding to other proteins.

Recombinant munc18a was found to be phosphorylated by a mixture of classic PKCs (PKCα, β and γ) in a cell-free system. This phosphorylation of munc18a inhibited its interaction with syntaxin [34]. In addition, munc18c isolated from parotid acinar cells was phosphorylated in vitro by the catalytic subunit of PKC [35]. The authors also showed that treatment of parotid acinar cell plasma membranes induced displacement of munc18c from the plasma membrane. We showed that munc18c is robustly phosphorylated in vitro but that PKCζ is not directly responsible. Phosphorylation of munc18c 338 was significantly lower than phosphorylation of munc18c 295. Thus removal of the PKCζ-interaction site from munc18c markedly decreased the phosphorylation. This indicates that either there is more than one phosphorylation site in munc18c, one of which resides in the PKCζ-interaction site region, or that munc18c 338 bound the relevant kinase less strongly. PKCζ is well known to bind other kinases and to deliver them to target sites [20]. Either way the results further emphasise the importance of the PKCζ-interaction site of munc18c. The phosphorylation of munc18c opens up other avenues for its regulation.

In conclusion, we have identified a physiological association between munc18c and PKCζ that is enhanced by insulin. Disruption of PKCζ binding to munc18c inhibited insulin-stimulated glucose uptake and GLUT4 translocation to the plasma membrane. These results raise the prospect that insulin controls the clamping action of munc18c through PKCζ, thereby identifying a connection between an upstream insulin-regulated kinase and a component of the GLUT4 trafficking machinery.

Acknowledgements This work was supported by Diabetes UK.

References

1. Farese RV (2002) Function and dysfunction of aPKC isoforms for glucose transport in insulin-sensitive and insulin-resistant states. Am J Physiol Endocrinol Metabol 283:E1–E11
2. Bandyopadhyay G, Standaert ML, Sajan MP et al (2004) Protein kinase C-lambda knockout in embryonic stem cells and adipocytes impairs insulin-stimulated glucose transport. Mol Endocrinol 18:373–383
3. Hajduch E, Litherland GJ, Hundal HS (2001) Protein kinase B (PKB/Akt)—a key regulator of glucose transport? FEBS Lett 492:199–203
4. Whiteman EL, Cho H, Birnbaum MJ (2002) Role of Akt/protein kinase B in metabolism. Trends Endocrinol Metab 13:444–451
5. Khan AH, Pessin JE (2002) Insulin regulation of glucose uptake: a complex interplay of intracellular signalling pathways. Diabetologia 45:1475–1483
6. Chiang SH, Baumann CA, Kanzaki M et al (2001) Insulin-stimulated GLUT4 translocation requires the CAP-dependent activation of TC10. Nature 410:944–948
7. Foster LJ, Klip A (2000) Mechanism and regulation of GLUT-4 vesicle fusion in muscle and fat cells. Am J Physiol Cell Physiol 279:C877–C890
8. Watson RT, Kanzaki M, Pessin JE (2004) Regulated membrane trafficking of the insulin-responsive glucose transporter 4 in adipocytes. Endocr Rev 25:177–204
9. Elmendorf JS (2002) Signals that regulate GLUT4 translocation. J Membr Biol 190:167–174
10. Min J, Okada S, Kanzaki M et al (1999) Synip: a novel insulin-regulated syntaxin 4-binding protein mediating GLUT4 translocation in adipocytes. Mol Cell 3:751–760
11. Thurmond DC, Ceresa BP, Okada S, Elmendorf JS, Coker K, Pessin JE (1998) Regulation of insulin-stimulated GLUT4 translocation by Munc18c in 3T3L1 adipocytes. J Biol Chem 273:33876–33883
12. Tamori Y, Kawanishi M, Niki T et al (1998) Inhibition of insulin-induced GLUT4 translocation by Munc18c through interaction with syntaxin4 in 3T3-L1 adipocytes. J Biol Chem 273:19740–19746
13. Tellam JT, Macaulay SL, McIntosh S, Hewish DR, Ward CW, James DE (1997) Characterization of Munc-18c and syntaxin-4 in 3T3-L1 adipocytes. Putative role in insulin-dependent movement of GLUT-4. J Biol Chem 272:6179–6186
14. Pevsner J, Hsu SC, Scheller RH (1994) *n*-Sec1: a neural-specific syntaxin-binding protein. Proc Natl Acad Sci U S A 91:1445–1449
15. Spurlin BA, Thomas RM, Nevins AK et al (2003) Insulin resistance in tetracycline-repressible Munc18c transgenic mice. Diabetes 52:1910–1917
16. Samuels IS, Seibenhener ML, Neidigh KB, Wooten MW (2001) Nerve growth factor stimulates the interaction of ZIP/p62 with atypical protein kinase C and targets endosomal localization: evidence for regulation of nerve growth factor-induced differentiation. J Cell Biochem 82:452–466
17. Diaz-Meco MT, Municio MM, Frutos S et al (1996) The product of *par-4*, a gene induced during apoptosis, interacts selectively with the atypical isoforms of protein kinase C. Cell 86:777–786
18. Joberty G, Petersen C, Gao L, Macara IG (2000) The cell-polarity protein Par6 links Par3 and atypical protein kinase C to Cdc42. Nat Cell Biol 2:531–539
19. Izumi Y, Hirose T, Tamai Y et al (1998) An atypical PKC directly associates and colocalizes at the epithelial tight junction with ASIP, a mammalian homologue of *Caenorhabditis elegans* polarity protein PAR-3. J Cell Biol 143:95–106
20. Hodgkinson CP, Sale EM, Sale GJ (2002) Characterization of PDK2 activity against protein kinase B gamma. Biochemistry 41:10351–10359
21. Hodgkinson CP, Sale GJ (2002) Regulation of both PDK1 and the phosphorylation of PKC-zeta and -delta by a C-terminal PRK2 fragment. Biochemistry 41:561–569

22. Sale EM, Atkinson PG, Arnott CH, Chad JE, Sale GJ (1999) Role of ERK1/ERK2 and p70S6K pathway in insulin signalling of protein synthesis. FEBS Lett 446:122–126
23. Lim S-N, Bonzelius F, Low SH, Wille H, Weimbs T, Herman GA (2001) Identification of discrete classes of endosome-derived small vesicles as a major cellular pool for recycling membrane proteins. Mol Biol Cell 12:981–995
24. Arnott CH, Sale EM, Miller J, Sale GJ (1999) Use of an antisense strategy to dissect the signalling role of protein–tyrosine phosphatase alpha. J Biol Chem 274:26105–26112
25. Sale EM, Atkinson PG, Sale GJ (1995) Requirement of MAP kinase for differentiation of fibroblasts to adipocytes, for insulin activation of p90 S6 kinase and for insulin or serum stimulation of DNA synthesis. EMBO J 14:674–684
26. Wei ML, Bonzelius F, Scully RM, Kelly RB, Herman GA (1998) GLUT4 and transferrin receptor are differentially sorted along the endocytic pathway in CHO cells. J Cell Biol 140:565–575
27. Bogan JS, McKee AE, Lodish HF (2001) Insulin-responsive compartments containing GLUT4 in 3T3-L1 and CHO cells: regulation by amino acid concentrations. Mol Cell Biol 21:4785–4806
28. Sajan MP, Bandyopadhyay G, Kanoh Y et al (2002) Sorbitol activates atypical protein kinase C and GLUT4 glucose transporter translocation/glucose transport through proline-rich tyrosine kinase-2, the extracellular signal-regulated kinase pathway and phospholipase D. Biochem J 362:665–674
29. Arribas M, Valverde AM, Burks D et al (2003) Essential role of protein kinase C zeta in the impairment of insulin-induced glucose transport in IRS-2-deficient brown adipocytes. FEBS Lett 536:161–166
30. Ijuin T, Takenawa T (2003) SKIP negatively regulates insulin-induced GLUT4 translocation and membrane ruffle formation. Mol Cell Biol 23:1209–1220
31. Lampson MA, Schmoranzer J, Zeigerer A, Simon SM, McGraw TE (2001) Insulin-regulated release from the endosomal recycling compartment is regulated by budding of specialized vesicles. Mol Biol Cell 12:3489–3501
32. Muller G, Ayoub M, Storz P, Rennecke J, Fabbro D, Pfizenmaier K (1995) PKC zeta is a molecular switch in signal transduction of TNF-alpha, bifunctionally regulated by ceramide and arachidonic acid. EMBO J 14:1961–1969
33. Moscat J, Diaz-Meco MT (2000) The atypical protein kinase Cs. Functional specificity mediated by specific protein adapters. EMBO Rep 1:399–403
34. Fujita Y, Sasaki T, Fukui K et al (1996) Phosphorylation of Munc-18/*n*-Sec1/rbSec1 by protein kinase C: its implication in regulating the interaction of Munc-18/*n*-Sec1/rbSec1 with syntaxin. J Biol Chem 271:7265–7268
35. Imai A, Nashida T, Shimomura H (2004) Roles of Munc18-3 in amylase release from rat parotid acinar cells. Arch Biochem Biophys 422:175–182